

The Stunning, Glass-Covered Resting Cyst of *Maryna umbrellata* (Ciliophora, Colpodea)

Wilhelm FOISSNER

Universität Salzburg, FB Organismische Biologie, Salzburg, Austria

Summary. *Maryna umbrellata* (Gelei, 1950) Foissner, 1993 is a colpodid ciliate common in ephemeral water bodies. Pure cultures were established and the resting cyst studied by light and electron microscopy, protease digestion of thin sections, and various cytochemical reactions shown by colour micrographs. The cyst of *M. umbrellata* belongs to the kinetosome-resorbing (KR) type and has a conspicuous glass cover described by Foissner *et al.* (2009). It is 100 μm across and the about 13 μm thick wall, which amounts for half of the total cyst volume, consists of four distinct layers: (i) the about 6 μm thick pericyst, which is composed of glass granules embedded in mucoproteins, and of a basal layer consisting of glycogen tubules about 20 nm across; (ii) the about 140 nm thick, electron-dense ectocyst, which is not digested by protease; (iii) the about 6 μm thick mesocyst, which is distinctly laminated and made of proteins; and (iv) the thin, about 500 nm thick endocyst, which is structureless and consists of glycoproteins. The meso- and endocyst are highly elastic, reducing their diameter by 50% when the encysted ciliate is removed. The cyst contents is dominated by up to 7 μm -sized “spongy globules” consisting of an electron-dense, proteinaceous matrix burrowed by electron-lucent strands of glycogen, providing the cyst with a curious, white-spotted appearance in the electron microscope. The small lipid droplets have a proteinaceous centre. The cyst plasm contains proteins and unstructured mucosubstances, which stain with alcian blue, and thus possibly originate from the decomposed mucocysts. This study suggests that ciliate resting cysts are much more diverse than indicated by literature data.

Key words: *Colpoda*, cyst cytochemistry, comparative ultrastructure of colpodid resting cysts, function of cyst layers, silicon in ciliates.

INTRODUCTION

The ability to form a dormant stage, usually called cyst or spore, provides micro-organisms with an endless life, while specific properties of the cyst wall are very likely important for the biogeographic range a species or population can occur (Foissner 1987, 2006; Gutiérrez

et al. 2001). Specific cyst properties must also strongly influence the occurrence or absence of a certain species under certain environmental conditions. It is thus surprising that current protistology shows only meagre interest in cyst research, although some progress has been made by ecologists (e.g., Jonsson 1994, Kim and Taniguchi 1997, Müller and Wünsch 1999, Müller *et al.* 2002, Endo and Taniguchi 2006, Weisse *et al.* 2008), biochemists (e.g., Nakamura and Matsusaka 1992, Wato *et al.* 2003, Tsutsumi *et al.* 2004, Yamasaki *et al.* 2004, Akematsu and Matsuoka 2005, Oda and Matsusaka 2005), and molecular biologists (e.g., Gutiérrez *et*

Address for correspondence: Wilhelm Foissner, Universität Salzburg, FB Organismische Biologie, Hellbrunnerstrasse 34, A-5020 Salzburg, Austria; e-mail: wilhelm.foissner@sbg.ac.at

al. 2001, Gallejas and Gutiérrez 2003, Sugimoto and Endoh 2008).

The species investigated in the present study belongs to the order Colpodida, a group of ciliates where cysts have been extensively studied because some species of the genus *Colpoda* are easily cultivated and very common in terrestrial habitats, such as mosses, grassland puddles, and soil (for reviews see, Wagtendonk 1955, Corliss and Esser 1974, Meier-Tackmann 1982, Foissner 1993, Gutiérrez and Martin-González 2002, Gutiérrez *et al.* 2003). However, much of the morphological work is rather incomplete, for instance, a clear semischematic presentation of the cyst wall and its genesis is not available for any *Colpoda* species.

We have shown in *Meseres corlissi*, an oligotrichous ciliate, which has chitin in the cyst wall, highly complex organic scales (lepidosomes) on the cyst surface, and five types of cyst wall precursors, that the knowledge on ciliate resting cysts is very limited (Foissner 2005; Foissner *et al.* 2005, 2006; Foissner and Pichler 2006). This is sustained by studies on the cysts of *Opisthonecta* (Calvo *et al.* 2003) and *Maryna umbrellata*, the species investigated in the present study: it produces silicon (glass) granules in the trophic state and deposit them on the surface of the cyst (Foissner *et al.* 2009), the meso- and endocyst show a high elasticity, the pericyst contains a layer of glycogen tubules, and the cyst contents is studded with curious storage bodies providing the cyst with a unique, white-spotted appearance in the electron microscope. Further peculiarities occur during cyst wall genesis, which will be described in a forthcoming paper. For instance, the ectocyst precursors are released via the parasomal sacs of the kinetids.

MATERIAL AND METHODS, TERMINOLOGY

Material and cultivation

Maryna umbrellata (Gelei, 1950) Foissner, 1993 was isolated from an ephemeral meadow pond in the Donnenberg Park near the so-called house of the hangman, Salzburg City, Austria.

Maryna umbrellata is a planktonic, rapidly swimming ciliate (Figs 4, 5), which reproduces in division cysts formed on the bottom of the cultivation dish. Inspection of the food vacuoles and crude experiments with potential food sources (heterotrophic and autotrophic flagellates, small ciliates) showed that *M. umbrellata* fed mainly on bacteria, while flagellates were taken sparsely; ciliates were rejected. Thus, about 20 specimens were isolated to set up a pure culture with French table water (Eau de Volvic) and some

crushed wheat kernels to stimulate growth of the natural bacterial flora. Cultures were grown at room temperature and were renewed each a week by transferring about 20 cells and a decaying wheat kernel into fresh medium.

Identification. The species was determined by live observation (bright field and interference contrast), silver impregnation, and scanning electron microscopy, as described by Foissner (1991) and shown in Figures 4 and 5.

Maryna umbrellata was insufficiently known when Foissner (1993) revised the genus. Thus, Foissner *et al.* (2002) redescribed *M. umbrellata* from Costa Rican and Australian populations. However, later investigations (this paper) showed that the resting cysts of the Austrian and Australian populations were rather different, suggesting the latter as an undescribed species. This matter will be treated in a separate publication. For the present study it is sufficient to know that the Austrian population represents the "true" *M. umbrellata*, as described by Gelei (1950) and reviewed in Foissner (1993).

Induction of encystment

After the logarithmic growth phase, when few dividing cells occurred, most specimens encysted rapidly, possibly due to the accumulation of excretory products produced by both the ciliates and the bacteria. Cysts were morphologically fully developed and thus possibly mature after one to two days. To be at the safe side, all investigations were performed on cysts older than 10 days.

Classic light and electron microscopic methods

Cysts were studied *in vivo* and various preparations, using bright field and interference contrast microscopy. *In vivo* measurements were conducted at magnifications of $\times 100$ – 1000 . Nine cysts were sectioned for transmission electron microscopy, and four of them were studied in detail. The images were digitalized and improved electronically.

For scanning electron microscopy (SEM), cysts were fixed in cacodylate-buffered osmium tetroxide (2% w/v) at pH 6 for 30 min., rinsed and cleaned with tap-water, and then transferred to a special preparation chamber, where they were dehydrated with a graded ethanol series and critical-point dried (Foissner 1991). Finally, specimens were mounted on a SEM-stub and gold sputtered. Observations were made with a Cambridge Stereoscan 250 (Cambridge Instruments, Cambridge, United Kingdom) operated at 20 kV. For transmission electron microscopy (TEM), resting cysts were fixed for 30 min. in a mixture of 10 ml glutaraldehyde (25% v/v), 6 ml aqueous osmium tetroxide (2% w/v) and 10 ml aqueous, saturated mercuric chloride. After three washes in tap-water, the specimens were transferred to glycid ether 100 (Epon 812, Serva, Heidelberg, Germany) *via* a graded ethanol series and propylene oxide. Flat embedding in aluminium weighing pans allowed specimens to be investigated light microscopically (up to $\times 400$) to select well-preserved individuals. Ultrathin sections were cut with a diamond knife mounted on a Reichert ultracut. Sections were viewed in a Zeiss EM 910 (Oberkochen, Germany), either unstained or, as usual, after staining with uranyl acetate followed by lead citrate (UL staining). Further, a series of sections was stained with bismuth subnitrate, as described by Hayat (1989). This method, which reveals polysaccharides, is referred to "bismuth stain" throughout the paper. One micrometer thick semithin sections were mounted on microscope slides by heat (120°C for 30 min.).

Cytochemistry

The cytochemical investigations were performed on unfixed cysts and/or cysts fixed with ethanol (95% w/v) or formalin (10% w/v), using the protocols and controls described in the literature cited below. Except for reactions on semithin sections and protease digestion of ultrathin sections, all tests were made on "free," complete cysts pipetted on a microscope slide or handled with the centrifuge (2000 r/min. for 30 s; 500 g). Stained, centrifuged cysts were used either in wet condition and/or prepared with the ordinary histological technic to permanent slides (embedding in albumen-glycerol → 100% ethanol → xylol → resin).

As the cysts were about 100 µm in size and the wall was at least 10 µm thick, most investigations were performed on wet cysts slightly to strongly squeezed and flattened between microscope slide and coverslip. This reveals the cyst structures very well and fosters the photographic documentation.

Carbohydrates and mucosubstances. Unfixed cysts were tested for chitin with Van Wisselingh's method, as described by Foissner *et al.* (2005), applying KOH-treatment 15 min. and 30 min.; fly wings served as control. The iodine tests were performed on unfixed cysts on microscope slides, using Lugol's solution and chlorinated-zinc-iodine (Romeis 1968). The classic Periodic Acid-Schiff reaction (PAS after Mc Manus) and the Bauer technique, both described in Romeis (1968), were performed on cysts fixed with 10% formalin and 95% ethanol, respectively, and on semithin sections made from cysts prepared for transmission electron microscopy. All methods gave similar results; Bauer's technique worked better when treatment with chromic acid was increased from 60 min. to 100 min. Aqueous, filtered alcian blue (1%, pH 5) was applied to trophic specimens and unfixed cysts on microscope slides. At the ultrastructural level, polysaccharids were revealed by bismuth staining, as described in Hayat (1989).

Proteins. These were revealed in formalin-fixed cysts with the acrolein-Schiff method, as described by Pearse (1968); starch grains from the culture medium served as a control. At the ultrastructural level, protease (from *Streptomyces griseus*; Sigma, Japan) was applied to unstained ultrathin sections, using the following protocol: Grids with sections were treated with H₂O₂ (5%) for 10 min. at room temperature and rinsed three times, 10 min. each, with distilled water. Then, the grids were incubated at 37°C in protease (0.3% in 0.05 M Na-cacodylate buffer) for 25 min. ("mild" digestion) or 50 min. ("strong" digestion). Finally, the grids were washed one time in distilled water for 10 min. at room temperature. The air-dried sections were studied without staining. This simple method provides valuable data both on the cyst wall and the cyst contents.

Lipids. These were revealed by sudan black (1% in 70% ethanol) applied to unfixed cysts on a microscope slide and in protease-treated sections as described above.

Glass. Hydrofluoric acid (HF) treatment, scanning electron microscope assisted X-ray microanalysis (EDAX), and energy filtered transmission electron microscopy (EFTEM) revealed that the pericyst of *M. umbrellata* contains countless silicon granules (Foissner *et al.* 2009). In the present paper, only HF-treated ultrathin sections are shown.

Terminology

General ciliate terminology follows Lynn (2008). Cyst terminology is according to Gutiérrez *et al.* (2003), Foissner (2005), and Foissner *et al.* (2005).

RESULTS

General description

The resting cyst of *M. umbrellata* is difficult to study *in vivo* and in whole mounts because of its large size and thick wall, whose components are more or less superimposed when the focal plane is in the cyst centre (Figs 6, 10, 14). On careful observation, most cyst layers recognizable in the transmission electron microscope can be seen also in the light microscope, especially when the cyst is squashed.

The resting cysts of *M. umbrellata* are in the size of the trophic specimens (Table 1): \bar{x} 102 × 102 µm and 105 × 96 × 96 µm, corresponding to volumes of about 555 366 µm³ and 504 792 µm³, respectively. The cysts are spherical to globular, those from environmental specimens are slightly larger (\bar{x} 109 µm) than those from specimens cultivated for a month (\bar{x} 102 µm); the latter shrink to 81 µm when prepared for transmission electron microscopy. The cysts are dark at low magnification (× 40) due to their strong light refractivity, and yellowish-brown at higher magnification (≥ × 100) due to the brownish pericyst. The cyst surface is smooth to rather distinctly faceted, both in environmental and cultivated specimens (Figs 1, 6, 7a, 14, 23–25). The number of faceted cysts increases with cyst age and in partially or completely dehydrated preparations (Figs 17, 19, 23–25, 31, 33). Further, the distinctness of the facets is influenced by cultivation, i.e., in some cultures most cysts are smooth or slightly faceted, while in other cultures most are slightly to distinctly faceted.

Thickness of the cyst wall

Comparative measurements of cyst wall thickness *in vivo* and in TEM sections reveal a substantial difference (Table 1): 8.3 µm vs. 13.3 µm. The high coefficients of variation indicate that part of this difference is caused by sections not being near the cyst centre, i.e., the wall becomes the thicker the more the section is outside the cyst centre. A second reason might be that the measurements are not based on the same material: the cysts used for TEM were from specimens cultivated for about one month, while those used for the *in vivo* measurements were from specimens cultivated over one year. Very likely, wall thickness decreased due to the long cultivation.

Thus, the notions on the thickness of the individual cyst layers must be considered in the light of this problem. However, there is no doubt that the cyst wall of *M.*

Table 1. Morphometric data on mature resting cysts of *Maryna umbrellata*. CV – coefficient of variation in %, *i* – number of cysts investigated, LM – light microscopy, M – median, Max – maximum, Min – minimum, n – number of individual structures investigated, SD – standard deviation, SE – standard error of mean, SEM – scanning electron microscopy, TEM – transmission electron microscopy.

| Characteristics ^a | Method | Unit | Mean | M | SD | SE | CV | Min | Max | n | <i>i</i> |
|---|--------|------|--------|--------|-------|------|------|-------|--------|-----|----------|
| Trophic specimens, width (OsO ₄ -fixed) | LM | µm | 105.1 | 100.0 | 19.2 | 3.3 | 18.3 | 75.0 | 140.0 | 34 | 34 |
| Trophic specimens, height (OsO ₄ -fixed) | LM | µm | 95.8 | 90.0 | 13.8 | 2.4 | 14.4 | 75.0 | 125.0 | 34 | 34 |
| Cysts, diameter in vivo (from environmental specimen) | LM | µm | 109.3 | 110.0 | 10.7 | 2.8 | 9.8 | 90.0 | 128.0 | 15 | 15 |
| Cysts, diameter in vivo (from cultivated specimens) | LM | µm | 102.5 | 100.0 | 8.8 | 1.9 | 8.6 | 90.0 | 120.0 | 21 | 21 |
| Cysts, diameter after Epon embedding (cultiv. specimens) ^a | LM | µm | 80.8 | 82.5 | 8.6 | 1.0 | 10.6 | 65.0 | 100.0 | 69 | 69 |
| Pericyst, total thickness | TEM | µm | 5.7 | 5.5 | 1.0 | 0.3 | 17.1 | 4.4 | 7.7 | 9 | 9 |
| Basal layer, thickness | TEM | µm | 1.7 | 1.2 | 0.8 | 0.3 | 48.7 | 0.9 | 3.4 | 9 | 9 |
| Basal layer, diameter of tubules | TEM | nm | 20.0 | 20.0 | 5.1 | 0.7 | 25.4 | 11.0 | 36.0 | 57 | 9 |
| Ectocyst, thickness | TEM | nm | 140.0 | 122.0 | 65.3 | 21.8 | 46.7 | 71.0 | 286.0 | 9 | 9 |
| Mesocyst, thickness | TEM | µm | 6.5 | 6.0 | 1.7 | 0.6 | 26.2 | 4.2 | 9.4 | 9 | 9 |
| Mesocyst, number of dark layers | TEM | – | 12.4 | 13.0 | 1.9 | 0.7 | 15.6 | 8.0 | 15.0 | 9 | 9 |
| Bright zone between meso- and endocyst, thickness | TEM | nm | 272.0 | 167.0 | 184.9 | 82.7 | 68.0 | 106.0 | 500.0 | 5 | 5 |
| Endocyst, thickness | TEM | nm | 512.8 | 490.0 | 237.1 | 79.0 | 46.3 | 222.0 | 900.0 | 9 | 9 |
| Cyst wall, total thickness in vivo (cultiv. spec.) ^b | LM | µm | 8.3 | 8.0 | 1.4 | 0.5 | 16.4 | 6.0 | 11.0 | 23 | 23 |
| Cyst wall, total thickness without glass layer | TEM | µm | 9.3 | 8.7 | 3.0 | 1.0 | 32.0 | 5.3 | 14.3 | 9 | 9 |
| Cyst wall, total thickness with glass layer | TEM | µm | 13.3 | 12.8 | 3.2 | 1.1 | 24.1 | 8.7 | 18.6 | 9 | 9 |
| Spongy globules, length | TEM | µm | 4.3 | 4.4 | 1.1 | 0.2 | 24.5 | 2.5 | 6.3 | 45 | 9 |
| Spongy globules, width | TEM | µm | 3.8 | 3.7 | 0.9 | 0.1 | 24.5 | 2.1 | 5.8 | 45 | 9 |
| Spongy globules, number of bright areas | TEM | – | 29.0 | 60.5 | 10.5 | 1.6 | 36.4 | 12.0 | 53.0 | 46 | 9 |
| Spongy globules, max. length of a bright area | TEM | nm | 640.7 | 649.5 | 186.8 | 27.5 | 29.2 | 300.0 | 1333.0 | 46 | 9 |
| Lipid droplets, length | TEM | nm | 1161.1 | 1111.0 | 379.0 | 48.9 | 32.7 | 500.0 | 2000.0 | 60 | 7 |
| Lipid droplets, width | TEM | nm | 1049.0 | 1039.0 | 325.0 | 42.0 | 31.0 | 500.0 | 1733.0 | 60 | 7 |
| Silicon granules, length | SEM | nm | 813.9 | 812.0 | 313.0 | 28.0 | 38.5 | 333 | 1667.0 | 129 | 9 |
| Silicon granules, width | SEM | nm | 688.2 | 689.0 | 249.0 | 23.0 | 36.2 | 235 | 1481.0 | 129 | 9 |

^a From three cultures embedded over a period of six months.

^b With glass layer, which amounts for about half of wall thickness.

Table 2. Cytochemical investigation of resting cysts of *Maryna umbrellata*. – no reaction, + slight reaction, ++ distinct reaction, +++ strong reaction, PAS – Periodic Acid-Schiff reaction, TEMS – thin sections as used for transmission electron microscopy, UL – uranyl acetate and lead citrate-stained thin sections.

| Structures investigated | Carbohydrates and mucosubstances | | | | Proteins | | | Lipids | | Glass ^a |
|-------------------------|----------------------------------|----------------------|--------|--------|-----------------|-------------|----------|----------------------------|-------------|--------------------|
| | UL-stained TEMS | Bismuth-stained TEMS | Chitin | Iodine | PAS | Alcian blue | Acrolein | Protease digestion of TEMS | Sudan black | Hydrofluoric acid |
| Glass granules | ++ | ++ | - | + | - | +++ | + | - | - | +++ |
| Basal layer | ++ | ++ | - | - | ++ ^b | - | - | - | - | - |
| Ectocyst | +++ | +++ | - | ? | ? | ? | ? | - | - | - |
| Mesocyst | + | ++ | - | - | - | - | ++ | ++ | - | - |
| Endocyst | + | + | - | - | + | - | + | + | - | - |
| Spongy globules | + | ++ | - | + | + | - | ++ | ++ | - | - |
| Lipid droplets | + | ++ | - | - | - | - | + | + | ++ | - |
| Cytoplasm | + | + | - | + | + | ++ | + | + | - | - |

^a For details, see Foissner *et al.* (2009).

^b Clearly recognizable only in semithin sections (Fig. 25).

umbrellata is extraordinarily thick, viz., about 10 μm and thus makes up almost 50% of the total cyst volume (Fig. 53)!

Pericyst (Figs 1–3, 6–12, 14, 15, 19, 20, 23–25, 31–36, 38–40; Tables 1, 2)

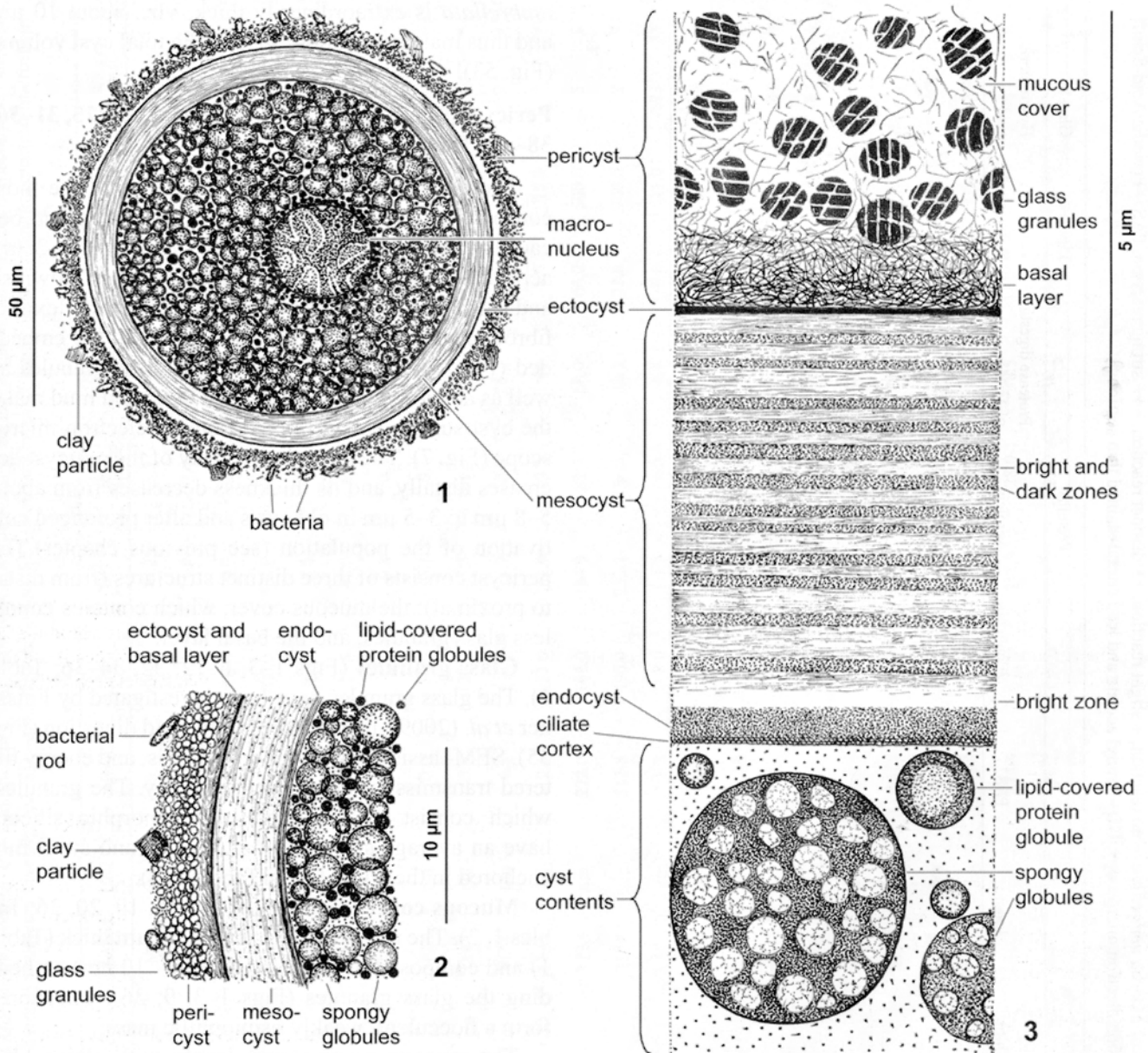
The about 6 μm thick pericyst is one of the most conspicuous features of the cyst of *M. umbrellata* because it contains countless glass granules 0.5–2 μm across (Foissner *et al.* 2009). The pericyst is brownish and membranous because it consists of a very flexible, fibrous matrix in which the glass granules are embedded (Figs 1, 2, 6–12; Table 1). The glass granules as well as adhering environmental bacteria and mud make the cyst surface rough in the scanning electron microscope (Fig. 7). The structural density of the pericyst decreases distally, and its thickness decreases from about 5–8 μm to 3–5 μm in old cysts and after prolonged cultivation of the population (see previous chapter). The pericyst consists of three distinct structures (from distal to proximal): the mucous cover, which contains countless glass granules, and the basal layer.

Glass granules (Figs 1–3, 6–12, 32, 34–36; Table 1). The glass granules have been investigated by Foissner *et al.* (2009), using hydrofluoric acid digestion (Fig. 35), SEM- assisted X-ray microanalysis, and energy filtered transmission electron microscopy. The granules, which consist of biomineralized, amorphous silicon, have an average size of 814 \times 688 μm and are firmly anchored in the slime layer (Tables 1, 2).

Mucous cover (Figs 1–3, 9, 14, 15, 19, 20, 36; Tables 1, 2). The mucous cover is about 4 μm thick (Table 1) and composed of very fine fibres (< 10 nm) embedding the glass granules (Figs 1–3, 9, 36). The fibres form a flocculent, weakly osmiophilic mass.

The mucous cover stains deeply with alcian blue (Figs 14, 15; Table 2) and rather distinctly with acrolein (Figs 19, 20; Table 2), suggesting that it consists of acid mucopolysaccharides and proteins (mucoproteins).

Basal layer (Figs 2, 3, 11, 15, 23–25, 31–36, 38–40, 49; Tables 1, 2). The basal layer is attached to the distal surface of the ectocyst and passes into the mucous cover without sharp border. It has an average thickness of 1.7 μm (Table 1), stains ordinarily with UL and bismuth, and is composed of tortuous, strongly intertwined tubules with an average diameter of 20 nm (Figs 31–36, 38–40; Table 1). The tubules are densely packed in the proximal half of the layer, often forming a fibrogranular, slightly laminated mass (Figs 32, 36, 38).

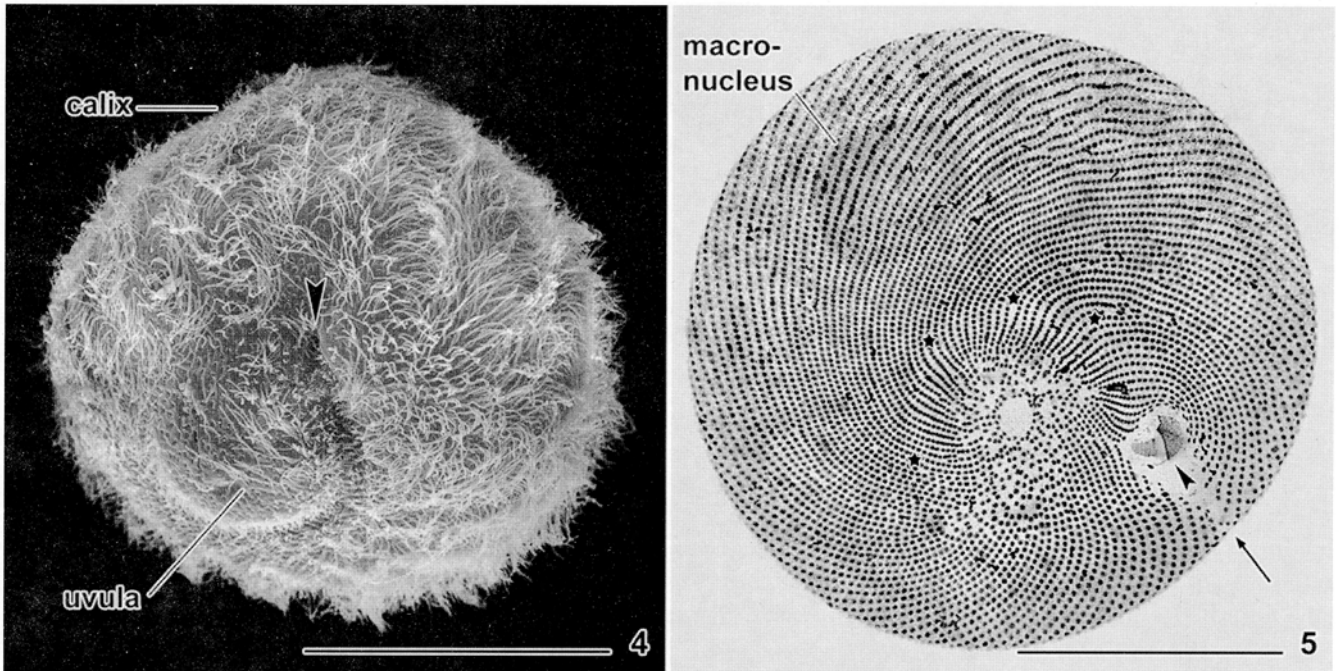


Figs 1–3. *Maryna umbrellata*, semischematic figures of resting cyst structures. Sizes are based on the average values shown in Table 1. 1, 2 – light microscopic overview and detail; 3 – cyst structure in the transmission electron microscope.

The basal layer, which is not digested by protease (Figs 33, 34, 49), stains rather intensely with PAS in semithin sections (Fig. 25; Table 2), suggesting that it consists of glycogen. In whole cyst mounts, the PAS reaction is lacking or weak, depending on the time of chromium acid treatment (Figs 23, 24).

Ectocyst (Figs 1–3, 11, 15, 32, 34, 36, 38, 49; Tables 1, 2)

The ectocyst has an average thickness of 140 nm and is thus not identifiable with certainty in the light microscope (Figs 2, 11, 15); actually, it is the thinnest and most electron-dense layer of the cyst wall of *M. umbrellata* (Table 1). In the transmission electron microscope, it is structureless, even at high magnification (Figs 36, 38).



Figs 4, 5. *Maryna umbrellata*, trophic specimens in the scanning electron microscope (4) and in a silver carbonate preparation (5). 4 – slightly oblique posterior view, showing the broadly conical body partited in calix and uvula by a deep furrow. The arrowhead marks the small mouth entrance at the boarder of calix and uvula; 5 – posterior polar view, showing the two oral ciliary fields (arrowhead) and the about 100 ciliary rows, which extend spirally, forming a suture on ventral side (arrow). The asterisks mark the boarder between calix and uvula. Scale bars: 50 μ m.

The composition of the ectocyst could be not clarified because it is too thin to be identifiable with the histochemical methods applied. Very likely, the ectocyst is not proteinaceous because it is not digested by protease (Figs 34, 49). As lipids are unlikely, it possibly consists of carbohydrates.

Mesocyst (Figs 1–3, 6, 8, 10, 11, 14, 15, 18, 19, 22, 24, 25, 28, 31–35, 37, 38, 41, 43, 49, 53; Tables 1, 2)

When focused on the cyst centre, most of the about 6 μ m thick mesocyst is hidden by the thick and comparatively massive pericyst (Figs 1, 2, 6, 10, 14; Table 1). The endocyst, which is only about 500 nm thick, is distinguishable from the mesocyst only in strongly squashed cysts (Figs 2, 8, 11). Both are bright and structureless and appear solid in the light microscope. However, when the cyst is opened by pressing the coverslip slightly with a needle, the meso- and endocyst show a surprising property: they detach from the ectocyst and shrink to about half the cyst diameter (Figs 8, 28). Frequently, the mesocyst splits during this procedure: the distal half remains attached to the ecto- and pericyst,

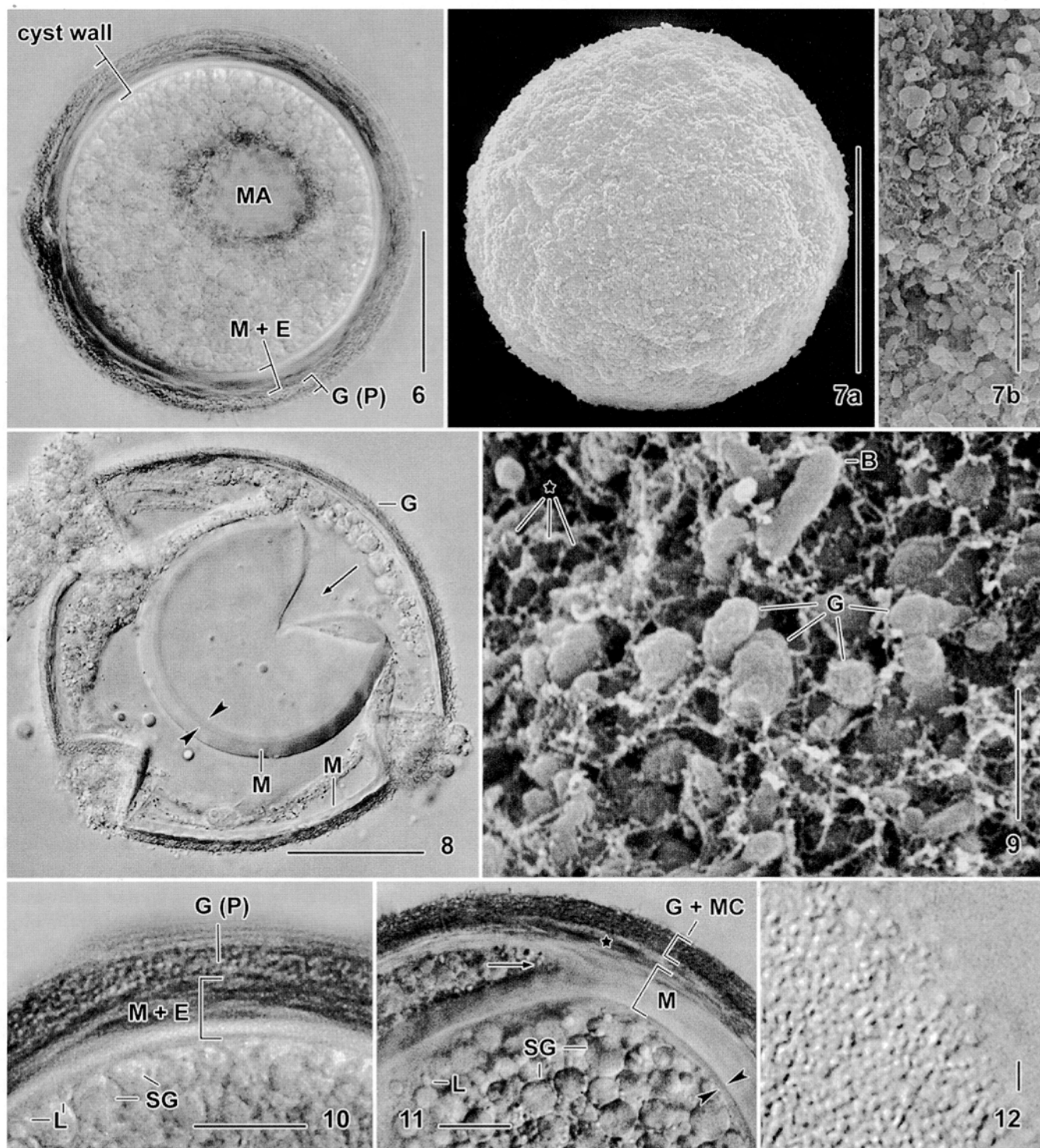
while the proximal half and the endocyst shrink as described before (Figs 8, 11, 15, 22).

The mesocyst is the thickest layer of the cyst wall (Table 1). In the transmission electron microscope, it consists of an average of 24 alternating layers with different electron density and fibro-granular fine structure. The thickness of the layers is different in the nine cysts analysed, and their distinctness increases in bismuth or hydrofluoric acid-treated sections (Figs 31, 32, 35, 37, 41).

The mesocyst stains with acrolein (Fig. 19) and is digested by protease (Figs 33, 34, 43, 49), showing proteins as a main component (Table 2). It does not react with iodine (Figs 18, 22), alcian blue (Fig. 15), PAS (Figs 24, 25), and sudan black (Fig. 28).

Bright zone between mesocyst and endocyst (Figs 3, 11, 24, 25, 32–34, 37, 41, 49; Tables 1, 2)

This part of the cyst wall has an average thickness of 272 nm and is thus not identifiable in the light microscope (Table 1). In the electron microscope, it is structureless and bright (Figs 3, 37). Frequently, this zone is



Figs 6–12. *Maryna umbrellata*, resting cysts in the light microscope (6, 8, 10–12) and in the SEM (7, 9). **6, 10** – overview and detail, showing that most of the thick mesocyst is covered by the opaque pericyst composed mainly of glass granules. The cysts are studded with “spongy globules”; **7, 9, 12** – the cyst surface is coarse and may be more or less faceted (7a). At higher magnification, the pericyst is composed of countless silicon granules (7b, 12) embedded in mucous material, which becomes distinct where the granules have been lost (9, asterisk); **8, 11** – squashed cysts showing the thick, split mesocyst (arrows), the thin endocyst (opposed arrowheads), and the glass layer. The asterisk marks the ectocyst and the basal layer. B – bacterial rod, E – endocyst, G – glass granules in mucous cover, L – lipid droplets, M – mesocyst, MA – macronucleus, MC – mucous cover, P – pericyst, SG – spongy globules. Scale bars: 2 μm (Figs 9, 12), 5 μm (7b), 10 μm (10, 11), and 40 μm (6–8).

hardly recognizable, i.e., not distinguishable from the mesocyst and endocyst, to which it might belong because the endocyst is thicker in the light than in the electron microscope (Figs 11, 24, 25, 32, 37, 41). The bright zone disappears in protease-treated sections because the mesocyst is digested and then appears as bright as the bright zone proper (Figs 33, 34, 49).

Endocyst (Figs 2, 3, 6, 11, 19, 24, 25, 32, 34, 35, 37, 41, 43, 49; Tables 1, 2)

The endocyst has an average thickness of 513 nm and is thus difficult to recognize in the light microscope (Fig. 11; Table 1). It is fairly distinctly separated from the mesocyst by the bright zone, which might belong to the endocyst (see above); proximally it is separated from the cortex of the encysted cell by a very thin, electron-lucent cleft (Figs 32, 41). A definite fine structure is lacking, i.e., it appears moderately dense and very finely granular (Figs 3, 32, 37, 41).

In semithin sections, the endocyst stains with PAS, suggesting carbohydrates as a main component (Fig. 25). In whole cyst mounts, there is also a reaction with acrolein (Fig. 19), indicating some protein (Table 2). This is sustained by the observation that it appears often considerably brighter in protease-treated sections (Figs 34, 43, 49). Thus, the endocyst is possibly a glycoprotein.

Cortex and cyst contents (Figs 1–3, 6, 10, 11, 15, 16, 18, 19, 21, 22, 24, 26–31, 33–35, 42–53; Tables 1, 2)

The cortex is maintained (Figs 3, 43), while the basal bodies and the cortical microtubules are decomposed.

In the light microscope, the following cyst inclusions are recognizable: the nuclear apparatus, “spongy globules” 2–7 μm across, lipid droplets $\leq 2 \mu\text{m}$ in size, and minute “crystals” distinctly sparkling under interference contrast illumination. Autophagous vacuoles were not seen neither in the light- nor in the electron microscope.

The nuclear apparatus is in or near the cyst centre (Figs 1, 6). No distinct changes are recognizable when compared with that of trophic specimens. However, it is covered with brownish “crystals” about 1 μm in size (Fig. 6). These “crystals,” which are also scattered in the cyst plasm, disappear after hydrofluoric acid treatment, suggesting that they consist of glass (Foissner *et al.* 2009). However, the electron microscopical investigations show an absence of silicon granules in the mature cyst plasm. Thus, the nature of the “crystals” remains obscure.

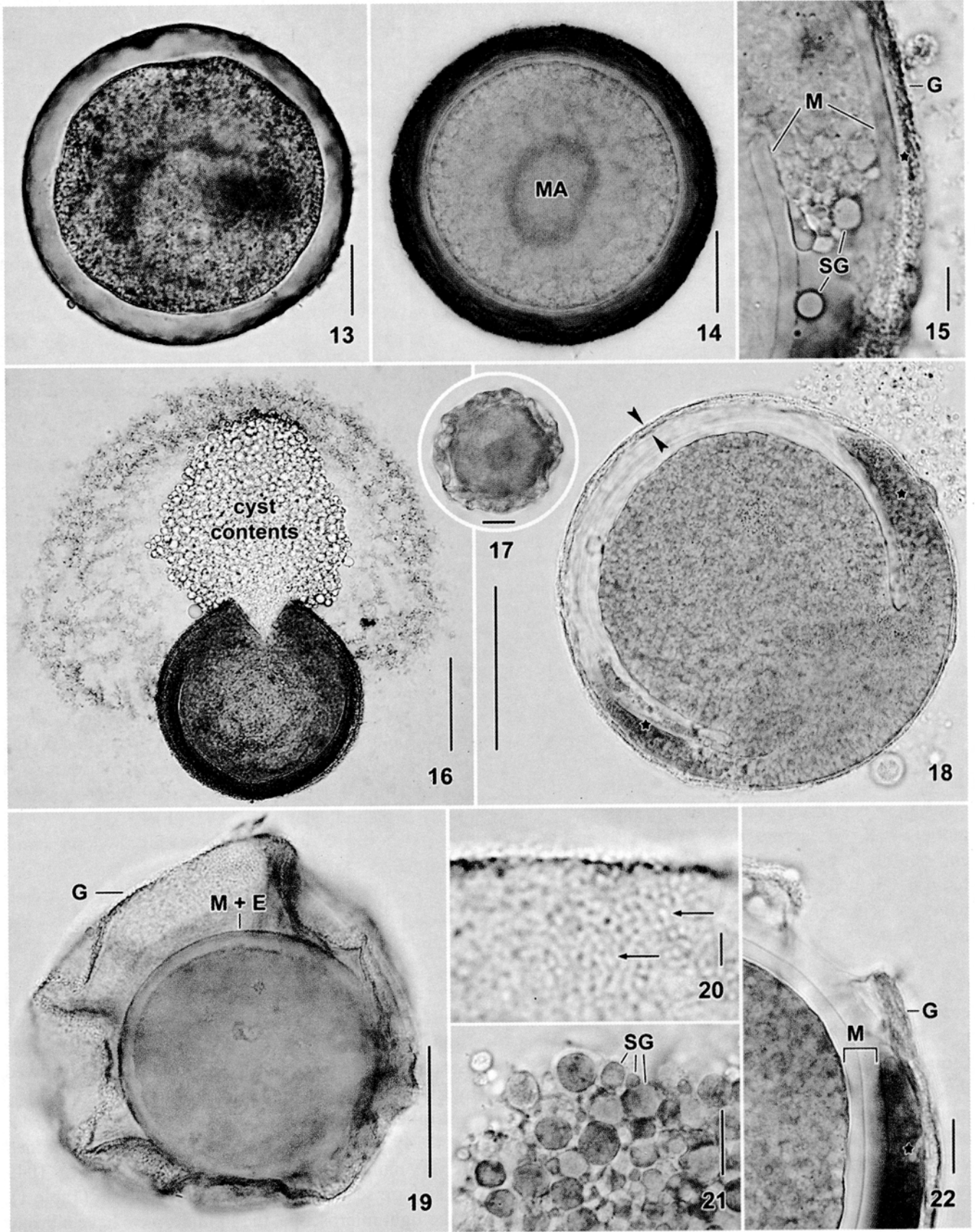
Spongy globules (Figs 1–3, 10, 11, 18, 19, 21, 24, 26, 27, 29, 31, 33–35, 42–52; Tables 1, 2). These are the most conspicuous cyst inclusions because they are very numerous and up to 7 μm across. They have a moderate light refractivity and often contain some granular material (Figs 1, 2, 6, 10, 11, 15, 21, 26, 29; Table 1). The spongy structure of the globules becomes distinct in cysts stained with Bauer’s PAS, where they swell due to the chromic acid treatment (Fig. 46).

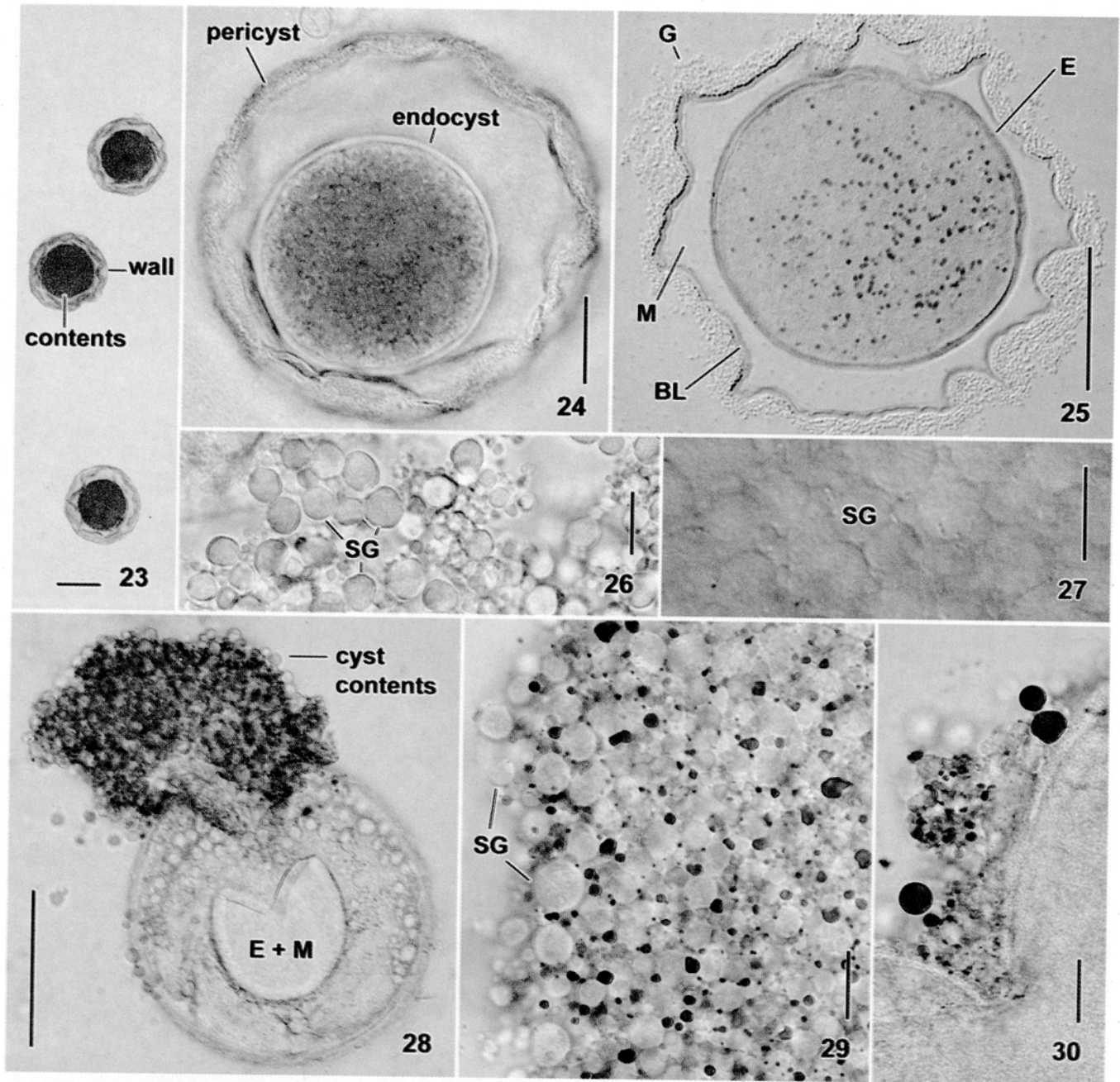
The spongy globules provide the mature cyst with a unique, white-spotted appearance in the transmission electron microscope (Fig. 53). In thin sections, the globules have an average size of $4.3 \times 3.8 \mu\text{m}$ and show an average of 29 bright areas (“unstained holes”) each with a size of about 600 nm (Table 1). Thus, a spongy globule has an area of about $13 \mu\text{m}^2$, of which $8 \mu\text{m}^2$ are occupied by the bright areas. The size of the globules and bright areas is highly variable, showing coefficients of variation between 24% and 36% (Table 1). Further, these globules are stable structures present also in cysts older than one month.

The complex fine structure of the spongy globules becomes recognizable when various stains and protein digestion are applied. Basically, the globules are membrane-bound vesicles consisting of an electron-dense matrix with scattered, small bright areas (Figs 3, 31, 35, 42, 44). In UL-stained sections, the matrix usually appears as a homogenous, finely granular mass (Figs 42, 44), while bismuth staining reveals polygonal, membrane-bound subunits, most having a bright area in the centre (Fig. 45). The bright areas appear structureless in UL-stained sections (Fig. 44), while conspicuously foamy in bismuth stains (Figs 45, 48).

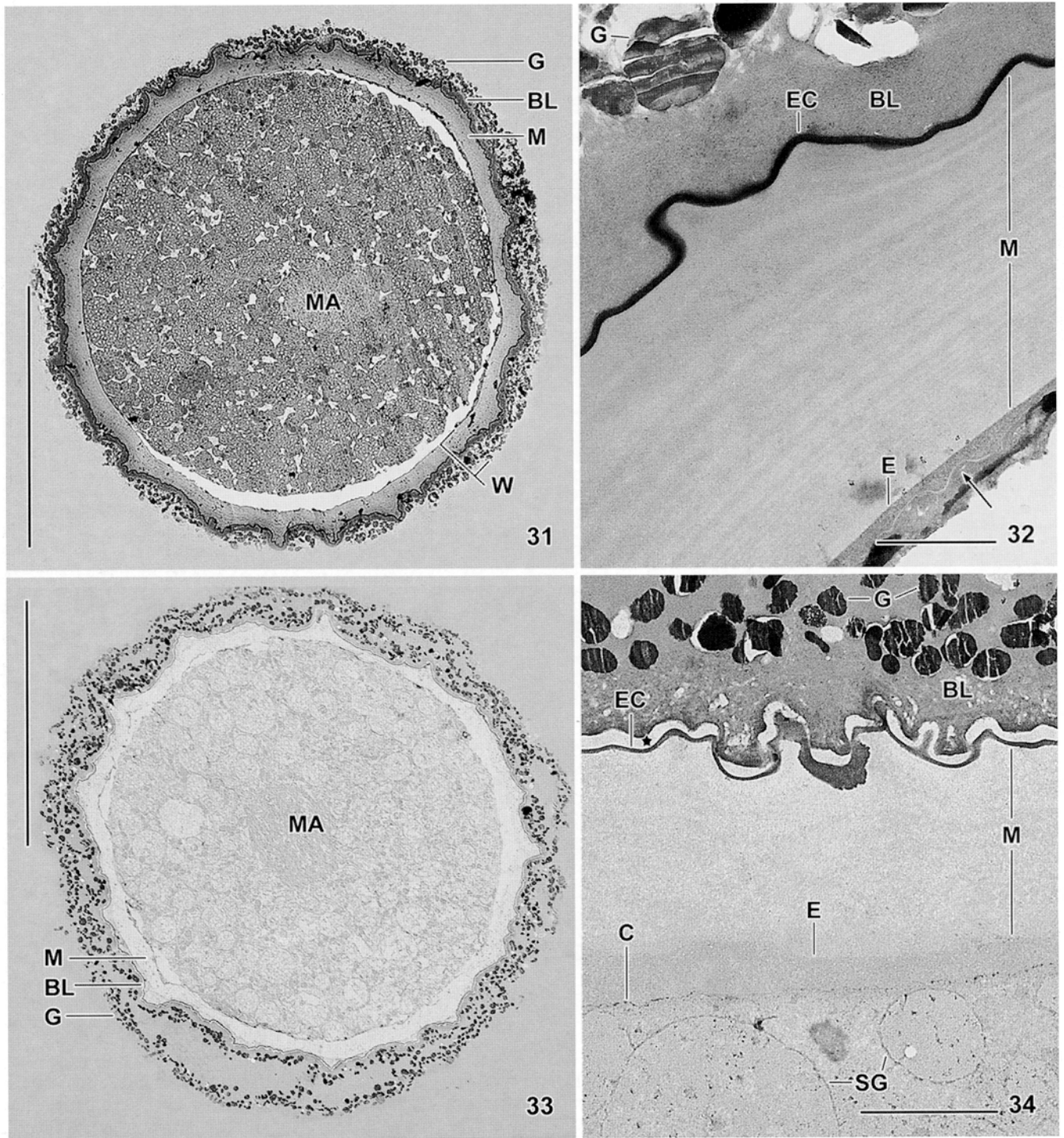
The spongy globules react to carbohydrate stains (iodine, Figs 18, 21; PAS, Figs 23–27; bismuth, Fig. 45; Table 2), protein stains (acrolein, Fig. 19) and, especially, to protease (Figs 33, 34, 43, 49–52). Protease digests the globules, except of the external and internal membranes and the unstained areas which now stand out as greyish spots from the whitish background (Figs 33, 34, 43, 49–52). These properties show that the spongy globules consist of glycoproteins in a special arrangement: the matrix is composed of proteins and burrowed by strands of glycogen (Table 2).

Lipid droplets (Figs 2, 3, 10, 11, 28–30, 35, 42, 44, 45, 47, 49, 51, 52; Tables 1, 2). These inclusions, which are very numerous, have an average size of $1161 \times 1049 \text{ nm}$ and are scattered through the cyst plasm (Table 1). In the light microscope, the lipid droplets have a bright

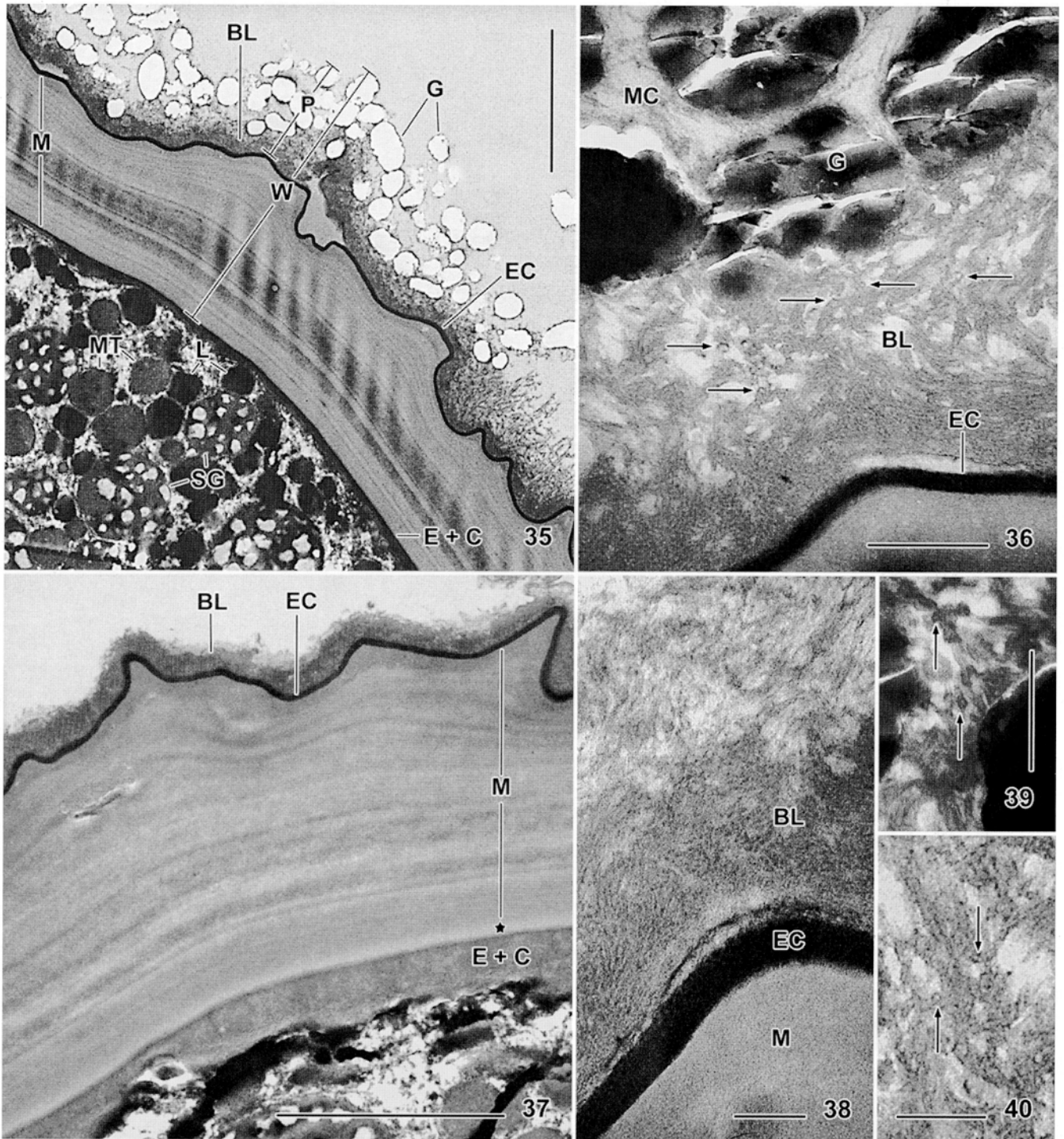




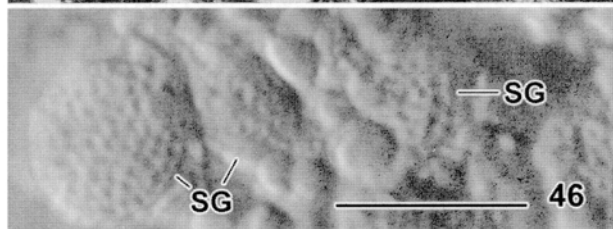
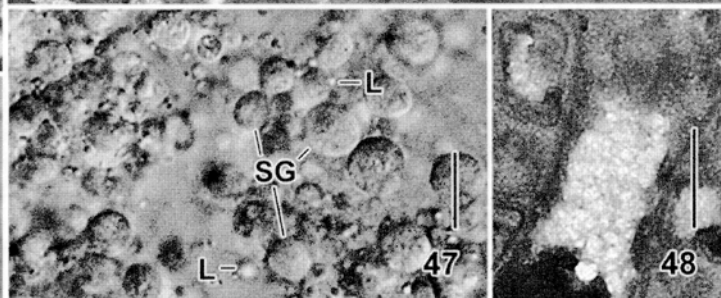
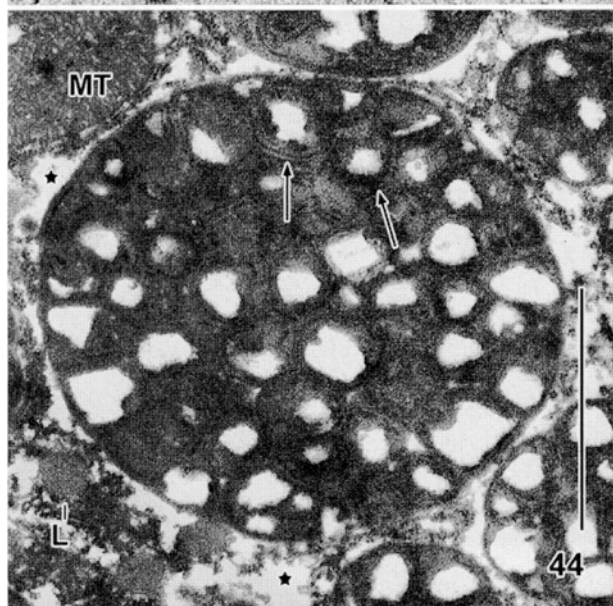
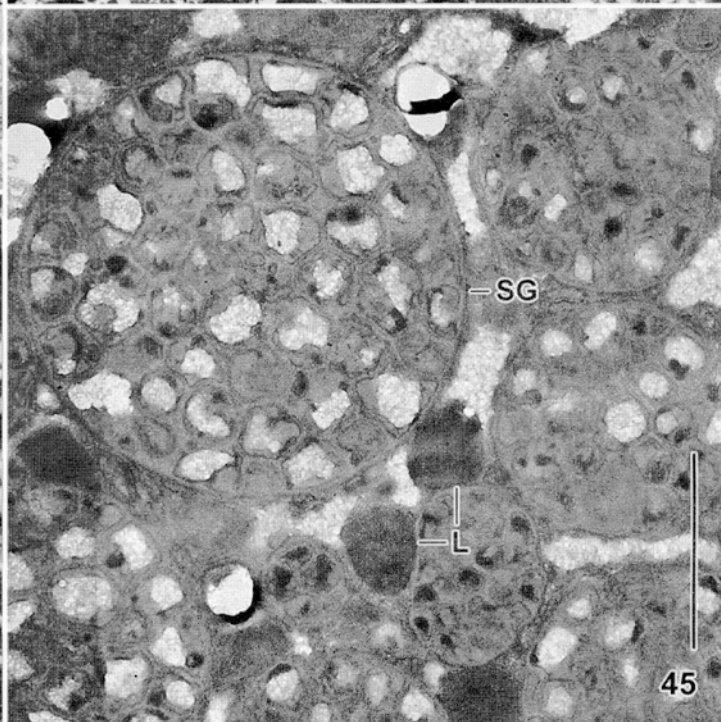
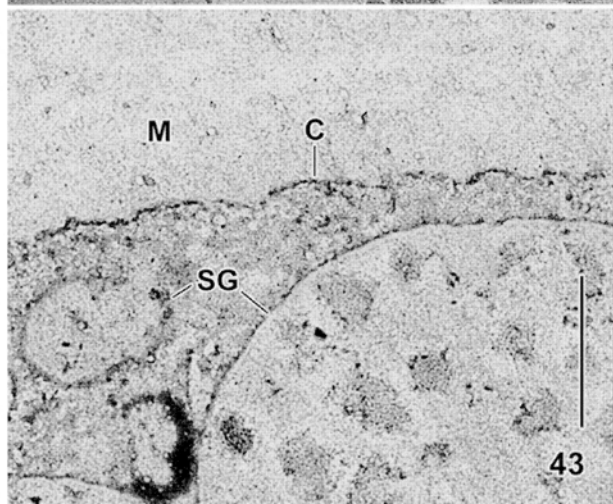
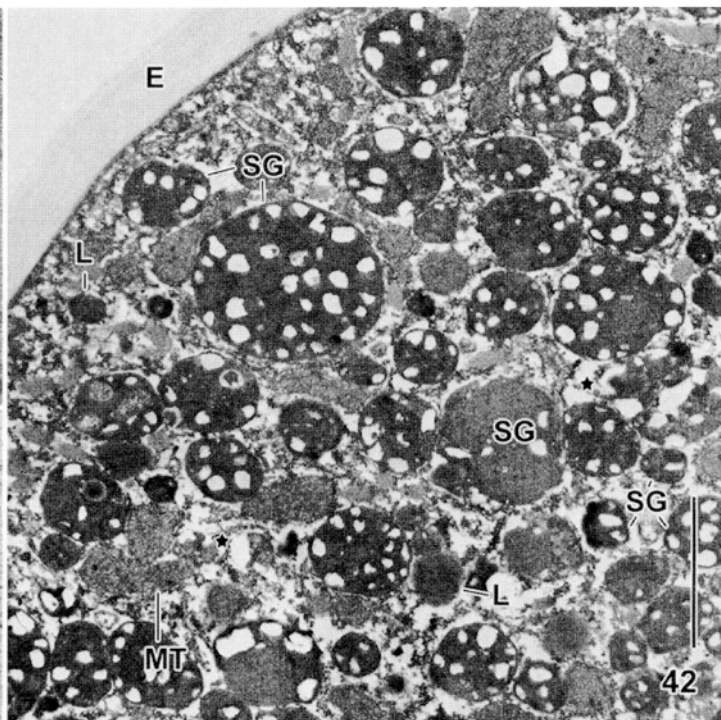
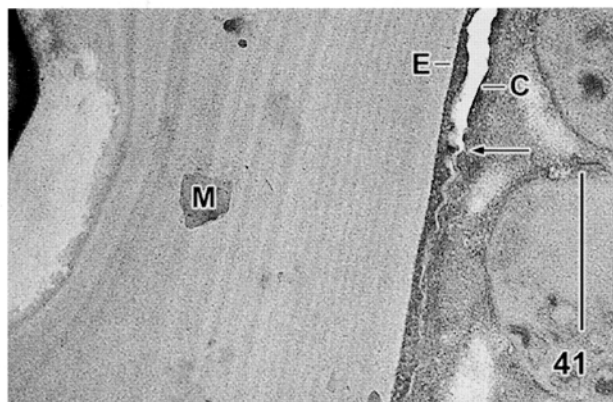
Figs 13–30. *Maryna umbrellata*, trophic (13) and cystic (14–30) specimens stained with alcian blue (13–16), iodine (17, 18, 21, 22), acrolein (19, 20), PAS (23–27), and sudan black (28–30). **13** – trophic cells extrude the mucocysts, swelling to a conspicuous envelope; **14, 15** – the periphery appears deeply stained when the focal plane is in cyst centre (14). Squashed cysts (15) show that only the glass layer is stained, while the basal layer and the ectocyst (asterisk) as well as the split mesocyst remain unstained; **16** – when the contents is squeezed out, a spongy mass stains, very likely decayed mucocysts; **17, 18, 21, 22** – iodine stains the glass layer lightly (17; 18, opposed arrowheads; 22) and the contents deeply, especially the “spongy globules” (17, 18, 21) and the plasm between the globules (18, 22, asterisks); **19, 20** – acrolein stains the whole cyst (19), except of the glass granules which appear colourless against the pink background (20, arrows); **23–27** – overviews (23, 24), details from squashed specimens (26, 27), and a sectioned cyst (25) show PAS positive reactions of the basal layer of the pericyst, the endocyst region, and the cyst contents; the endocyst and the basal layer are weakly stained in whole mounts (23, 24). The spongy globules stain lightly (26) but when 4% chromic acid is applied, the plasm between the globules stains rather deeply (27); **28–30** – alcoholic sudan black stains the lipid droplets (28, 29), several of which may unite to larger droplets when the preparation is squeezed (30). BL – basal layer, E – endocyst, G – glass layer, M – mesocyst, MA – macronucleus, SG – spongy globules. Scale bars: 2 μ m (Fig. 20), 10 μ m (15, 21, 22, 26, 27, 29, 30), 25 μ m (13, 14, 17, 24, 25, 28), and 50 μ m (16, 18, 19, 23).

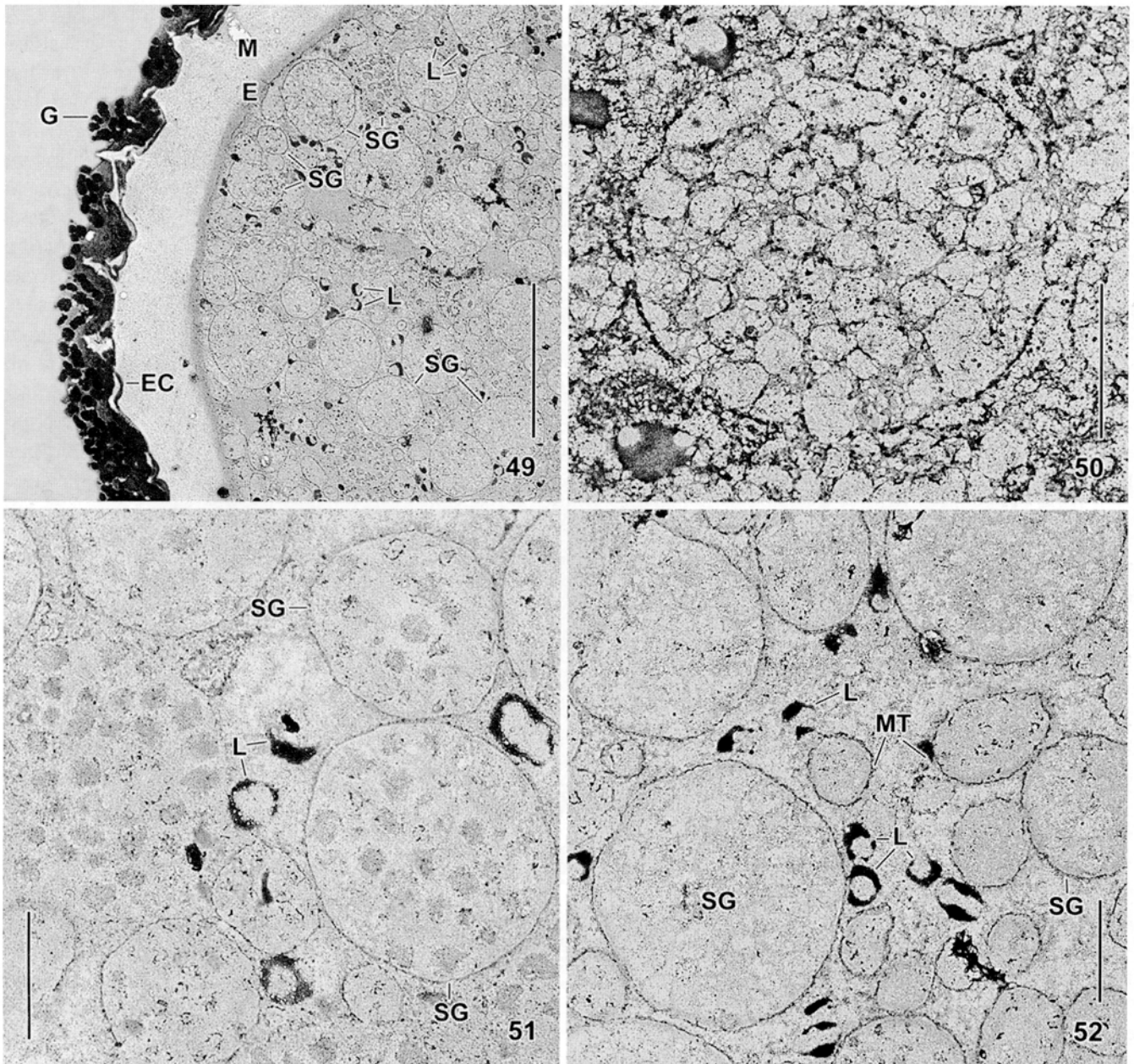


Figs 31–34. *Maryna umbrellata*, TEM micrographs of resting cysts. **31, 32** – overview and wall detail of bismuth stained sections. The wall is about 8 μm thick and consists of two conspicuous zones: the pericyst with glass granules and the thick, laminated mesocyst. The arrow in Fig. 32 marks a minute space between endocyst and ciliate cortex. The cyst contents are dominated by white-spotted “spongy globules,” which become very conspicuous at higher magnification (see Fig. 53); **33, 34** – overview and wall detail of unstained sections after protease digestion. Both the mesocyst of the cyst wall and the cyst contents appear light grey due to the digestion of proteins, while the ectocyst and the basal layer of the pericyst are as in Fig. 32, i.e., contain no or very few protein. The narrow space (asterisk) between ectocyst and basal layer is a shrinkage artifact. BL – basal layer, C – ciliate cortex, E – endocyst, EC – ectocyst, G – glass layer, M – mesocyst, MA – macronucleus, W – cyst wall. Scale bars: 1 μm (Fig. 32), 3 μm (34), and 40 μm (31, 33).



Figs 35–40. *Maryna umbrellata*, TEM micrographs of UL-stained cyst sections. **35** – cyst periphery of a section treated with hydrofluoric acid. The glass granules solvled and are thus electron lucent. *Maryna umbrellata* has a very thick pericyst and mesocyst, while ectocyst and endocyst are less than 1 μm thick; **36, 38–40** – details of the dense, structureless ectocyst (**36, 38**) and the pericyst. The latter consists of the mucous cover embedding the glass granules (**36**) and the basal layer, which is composed of intertwined tubules with a diameter of about 20 nm (**36, 39, 40**, arrows); **37** – high magnification of cyst wall. Note the thin, electron-dense ectocyst, the laminated mesocyst, and the narrow space between mesocyst and endocyst (asterisk). BL – basal layer, C – ciliate cortex, E – endocyst, EC – ectocyst, G – glass granules, L – lipid droplets, M – mesocyst, MC – mucous cover, MT – mitochondria, P – pericyst, SG – spongy globules, W – cyst wall. Scale bars: 200 nm (Figs 38–40), 400 nm (**36**), and 4 μm (**35, 37**).





Figs 41–52. *Maryna umbrellata*, light (46, 47) and electron microscopical (41–45, 48–52) structure of the cyst contents after staining with UL (42, 44) or bismuth (41, 45, 48) and in protease digested, unstained sections (43, 49–52); 41 – the thin endocyst and the cortex of the ciliate are electron-dense and sometimes separated by a narrow shrinkage space (arrow; cp. Fig. 32); 42, 44, 46, 47 – the cyst contents consists mainly of “spongy globules” and lipid droplets (47). The spongy globules, whose polygonal substructure is sometimes recognizable in the TEM (44, arrows) and after prolonged chromic acid treatment in the PAS reaction (46), consist of an electron-dense matrix and electron-lucent, structureless “holes” (42, 44). The lipid droplets and the cyst plasm (42, 44, asterisks) appear structureless; 45, 48 – when stained with bismuth, both the electron-lucent areas in and between the spongy globules and lipid droplets show a foamy structure, indicating the presence of polysaccharides. The matrix of the spongy globules shows a polygonal pattern, each polygon usually having an electron-lucent, foamy centre; 43, 49–52 – sections treated with protease for 25 min. (43, 49–51) and 50 min. (52) are much less electron-dense than ordinary sections (31–34, 49) because most substance of the mesocyst and the spongy globules has been digested. Mild digestion leaves back the contents of the “holes” of the spongy globules (43, 51) and, occasionally, the membranes surrounding their subunits (50). Strong digestion leaves back mainly the membranes (52). The lipid droplets have a proteinaceous centre (49, 51, 52). C – ciliate cortex, E – endocyst, EC – ectocyst, G – glass granules, L – lipid droplets, M – mesocyst, MT – mitochondria, SG – spongy globules. Scale bars: 500 nm (Fig. 48), 1 μ m (41, 43, 44, 49), 2 μ m (42, 45, 50–52), and 10 μ m (46, 47).

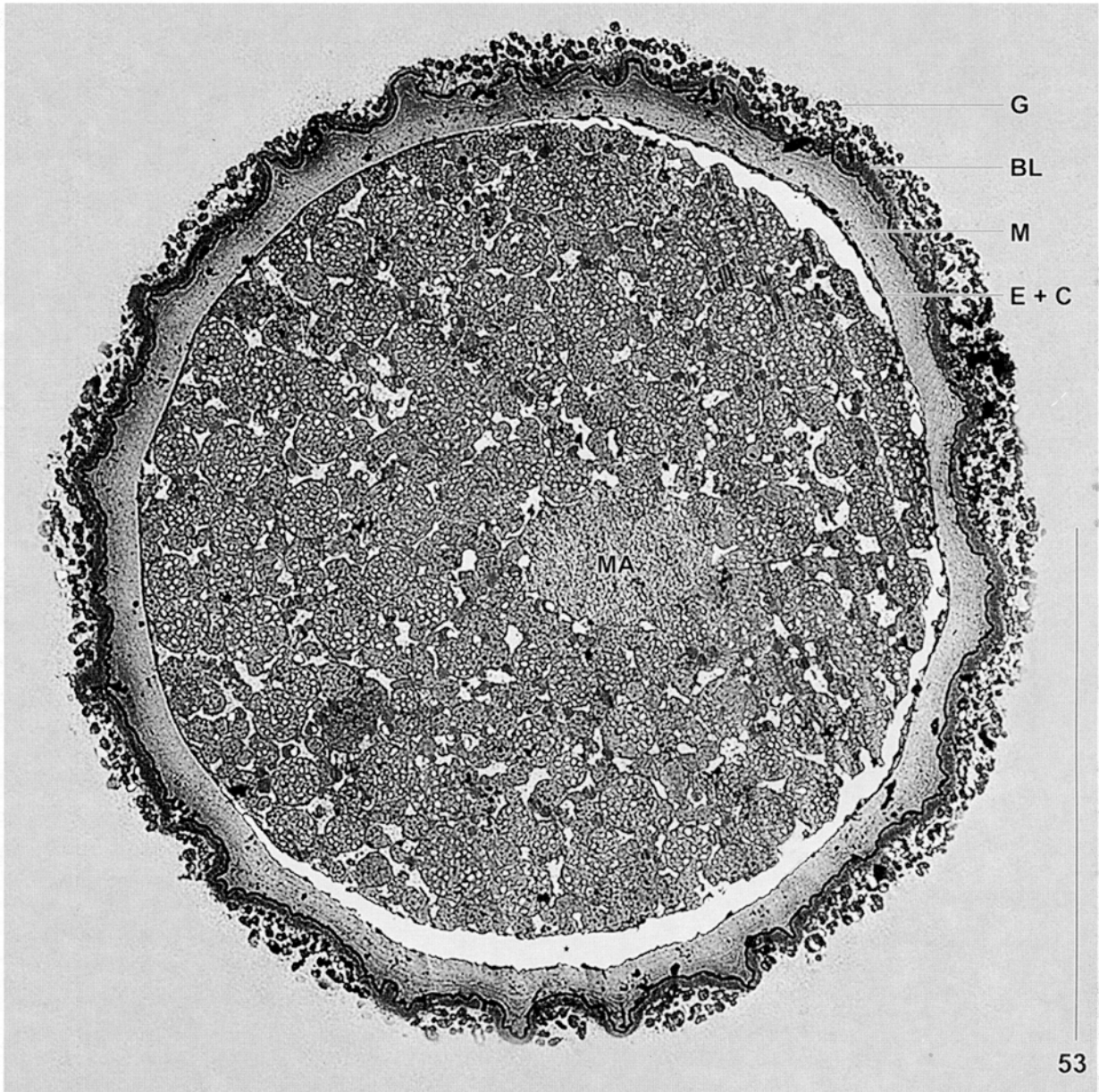


Fig 53. *Maryna umbrellata*, transmission electron micrograph of a resting cyst, showing the cover of glass granules and many peculiar, white-spotted globules within the cyst. These conspicuous storage products are produced by unstained, tortuous strands of glycogen embedded in an electron-dense, proteinaceous matrix. Note that the volume of the thick cyst wall is, indeed, the same as that of the encysted cell. This demonstrates impressively the significance of the wall in the life cycle. Very likely, the wall does not only protect the cell from environmental stress but also plays an important role in the environment and in initiating the excystment process. The asterisk marks shrinkage space between the encysted cell and the cyst wall. BL – basal layer, E + C – ectocyst and cortex, G – glass granules, M – mesocyst, MA – macronucleus. Scale bar 50 μm .

shimmer (Figs 2, 10, 11, 29). They are rather deeply stained with UL and bismuth, but are structureless in the transmission electron microscope (Figs 35, 42, 44, 45).

In vivo, the lipid droplets stain deeply with sudan black, showing the presence of lipids (Figs 28–30; Ta-

ble 2). This is in accordance with their appearance in the transmission electron microscope (see above). However, protease digestion reveals a more complex structure: the droplets are composed of proteins covered with a rather thin lipid layer (Figs 49, 51, 52; Table 2).

Cyst plasm (Figs 16, 18, 22, 27, 42, 44, 45, 48–52; Table 2). The resting cyst of *M. umbrellata* is studded with comparatively large glycoprotein globules (~ 5 µm) and minute, lipid-covered protein droplets (~ 1 µm). Thus, few space remains for other inclusions (e.g., mitochondria) and fluid cytoplasm, which appears bright or greyish in UL-stained sections (Figs 42, 44). However, when stained with bismuth, the cytoplasm shows a foamy structure highly similar to that of the bright areas in the spongy globules (Figs 45, 48). Thus, the fluid cytoplasm contains unstructured polysaccharids. This would agree with the light microscopic observations on squashed cysts, which release spongy material stainable with alcian blue (Fig. 16) and a fluid becoming deep orange when reacting with iodine (Figs 18, 22) and red in PAS stains (Fig. 27). Further, the plasm becomes lighter in sections treated with protease, showing the presence of proteins (Figs 49–52; Table 2).

DISCUSSION

Any discussion on ciliate resting cysts is limited by the simple fact that very few detailed studies are available on the intraspecific variability and on the interspecific diversity, i.e., the cysts of less than 40 species have been investigated in some detail (Gutiérrez *et al.* 2003). The intraspecific and environmental variability can be considerable, as shown by Weisse *et al.* (2008) in *Meseres corlissi* and by Foissner *et al.* (2007) in *Halteria grandinella*, a common cosmopolite which, however, very likely consists of several sibling species (Katz *et al.* 2005). Our overall ignorance on ciliate resting cysts is best demonstrated by the present and a former study (Foissner *et al.* 2009), where glass has been reported for the first time as a main component of the cyst wall.

Cyst morphology: within family comparison

The family Marynidae contains four genera with a total of 24 species (for reviews, see Foissner 1993 and Foissner *et al.* 2002). Electron microscopical investigations on their cysts are lacking, but light microscopical observations are available from five species and were reviewed by Foissner (1993) and Foissner *et al.* (2002). The cyst of *M. galeata* is dull red and covered with minute sand grains. The cyst of *M. atra* is possibly similar to that of *M. umbrellata*. The cysts of *M. umbrellata* from Europe (described here) and Australia (described in Foissner *et al.* 2002) are possibly quite different. The

latter has an only 1 µm thick meso- and endocyst, while the slimy pericyst contains up to 5 µm-sized globules similar to those found in some *Colpoda* species (see below). Such globules cover also the cyst of *Mycterothrix tuamotuensis*, while the cyst of *M. erlangeri* is covered by discs and tri-armed structures reminiscent of spongy “tri-rays.” When the present data are added, a considerable diversity of the marynid resting cysts becomes likely. Possibly, this diversity is related to their habit, ranging from ephemeral ponds to permanent waters, from freshwater to highly saline inland waters, and from ordinary to highly saline coastal and desert soils (for reviews, see Foissner 1993 and Foissner *et al.* 2002).

Cyst morphology: comparison with genus *Colpoda*

The genus *Colpoda* belongs to the family Colpodiidae which consists of eight genera with a total of about 50 species, of which we have light microscopical data on the resting cysts from 21 species (for reviews, see Foissner 1993, Foissner *et al.* 2002). These species show at least 12 (!) main cyst types. Unfortunately, electron microscopical investigations are available only from *C. magna*, *C. minima*, *C. lucida*, *C. cucullus*, *C. inflata*, and *C. steinii*.

A comparison of the resting cysts of the Marynidae and Colpodiidae is appropriate because these families are closely related, both genetically (Dunthorn *et al.* 2008) and morphologically (Foissner 1993), differing mainly in the location of the oral apparatus: in anterior (Colpodiidae) vs. posterior (Marynidae) half of body. However, such comparison is difficult because the data are often incomplete and the interpretation of number and kind of cyst layers varies considerably. For instance, previous researchers did not distinguish between pericyst and ectocyst but added the former to the latter. Further, species were sometimes misidentified and previous light microscopical data neglected in the interpretation of the electron microscopical findings. Thus, my comparison is strongly influenced by the investigations on *M. umbrellata* and the re-interpretation of previous data.

Comparison with *C. magna*, as described by Foissner (1993) and Frenkel (1994). Basically, the cyst is similar to that of *M. umbrellata*, except for the following features: (i) The slimy pericyst is inconspicuous and lacks a glass cover, but possibly has a basal layer. (ii) The mesocyst tends to split into several distinct sheets, especially in old cysts. Although the mesocyst of *M. umbrellata* has many layers of different electron density, it never splits, not even in cysts older than three months. (iii) The somatic basal bodies are retained,

while resorbed in *M. umbrellata*. (iv) The cyst volume ($448,693 \mu\text{m}^3$) is distinctly lower than the volume of the morphostatic specimens ($992,868 \mu\text{m}^3$), while similar in *M. umbrellata*.

Comparison with *C. minima*, as described by Foissner (1993) and Diaz *et al.* (2003). This species is difficult to distinguish from *C. magna*, both genetically (Dunthorn *et al.* 2008) and morphologically, including the light microscopical structure of the resting cyst (Foissner 1993). However, at electron microscopic level, the cysts of *C. minima* and *C. magna* appear rather different, although the data of Diaz *et al.* (2003) are very incomplete and possibly from young, not yet mature cysts. Compared to *M. umbrellata*, the cyst of *C. minima* (i) lacks a distinct pericyst, except of a thin slime cover; (ii) probably has a much thicker ectocyst; (iii) lacks any lamination of the mesocyst (Diaz *et al.* 2003), which splits into several distinct sheets in old cysts (Foissner 1993); and (iv) the cyst volume ($220,781 \mu\text{m}^3$) is rather distinctly lower than the volume of the morphostatic specimens ($331,488 \mu\text{m}^3$). No data are available whether or not the somatic basal bodies are resorbed.

Comparison with *C. cucullus*, as described by Janisch (1980) and Foissner (1993). Possibly, only Janisch (1980) identified the species correctly, while other *C. cucullus* populations belong either to *C. lucida* or *C. inflata* (see these species below). According to the investigations of the authors mentioned above, the cyst walls of *M. umbrellata* and *C. cucullus* differ in the following features: (i) pericyst complex vs. a simple mucous layer; (ii) mesocyst stable vs. splitting in several distinct sheets in old cysts; (iii) somatic cilia and basal bodies resorbed vs. retained (Foissner 1993, p. 155); (iv) cyst volume equal vs. slightly lower ($50,939 \mu\text{m}^3$) than in morphostatic specimens ($73,267 \mu\text{m}^3$).

Comparison with *C. lucida*, as described by Kawakami and Yagiu (1963) and Foissner (1993). The Japanese authors identified their population as *C. cucullus*, according to the state of art. However, *C. cucullus* was split into two species by Foissner (1993; and unpubl. data): *C. cucullus* (with inconspicuous mucocysts, without cyst lepidosomes, mesocyst split in old cysts) and *C. lucida* (with conspicuous mucocysts and cyst lepidosomes with hexagonal fine structure, mesocyst does not split). The cyst wall of *C. lucida* is similar to that of *M. umbrellata* but thinner, while the ectocyst is comparatively thick (see Fig. 7 in Kawakami and Yagiu 1963). Thus, the main difference is the pericyst, which contains glass granules in *M. umbrellata*, while lepidosomes in *C. lucida*. The cyst volume is conspicuously

lower ($38,772 \mu\text{m}^3$, $124,725 \mu\text{m}^3$ when the pericyst is included) than that of trophic cells ($214,776 \mu\text{m}^3$). No solid data are available whether or not the somatic basal bodies are resorbed.

Comparison with *C. inflata*, as described by Foissner (1993) and Foissner (unpubl. TEM data). This species has, like *C. lucida* (see above), lepidosomes consisting of fine, highly intertwined tubules. Thus, the *C. cucullus* population studied by Chessa *et al.* (2002) could be a *C. inflata*. The population investigated by Martin-González *et al.* (1992a, b) lacks lepidosomes and thus cannot be *C. inflata*; a scanning micrograph (Fig. 1 in Martin-González *et al.* 1992b) indicates that it could be *C. maupasi*. Considering these problems, I briefly describe the cyst wall of *C. inflata* according to my unpublished data. The cyst wall of *C. inflata* is similar to that of *M. umbrellata* but thinner and differs in the following features: (i) pericyst with lepidosomes vs. glass granules; (ii) mesocyst without vs. with lamination; (iii) cyst volume ($4,846 \mu\text{m}^3$) conspicuously lower than that of trophic cells ($31,250 \mu\text{m}^3$) vs. about equal. No data are available whether or not the somatic basal bodies are resorbed.

Comparison with *C. steinii*, as described by Tibbs (1968), Ruthmann and Kuck (1985), and Foissner (1993). This minute species seems to have only two cyst layers: a thin, dense ectocyst and a moderately dense meso- or endocyst. However, the data of Tibbs (1968, Fig. 16) and Ruthmann and Kuck (1985, Fig. 4) can be interpreted also differently: ectocyst very thin, sloughs of membranous material forming the pericyst; a thin, compact mesocyst; and a thick, less dense endocyst. According to the data of the authors mentioned above, the cyst walls of *M. umbrellata* and *C. steinii* differ in the following features: (i) pericyst with glass granules vs. membranous material; (ii) meso- or endocyst possibly lacking in *C. steinii*; (iii) somatic cilia and basal bodies resorbed vs. retained; (iv) cyst volume equal vs. distinctly lower ($2,144 \mu\text{m}^3$) than that of morphostatic specimens ($6,782 \mu\text{m}^3$).

The critical analysis of the data shows a basic similarity of the cyst wall of *M. umbrellata* and *Colpoda* spp., possibly except of *C. steinii*: all have a pericyst; a very thin, dense ectocyst; a thick, less dense mesocyst which may split into several sharply contoured sheets in *Colpoda* spp.; and a thin, moderately dense endocyst. Most of the cyst wall diversity is associated with the pericyst, i.e., the most external layer: glass granules embedded in slime and a tubular basal layer in *M. umbrellata*; organic scales (lepidosomes) embedded in slime

in *C. lucida* and *C. inflata*; membranous material in *C. steinii*; and a more or less thick, simple slime layer in *C. magna*, *C. minima*, and *C. cucullus*. A further main difference concerns the somatic basal bodies: they are resorbed in *M. umbrellata*, while retained in several (*C. magna*, *C. cucullus*, *C. steinii*) or even all *Colpoda* species. *Maryna umbrellata* is also curious in that the cyst volume is about the same as in morphostatic specimens. However, the same is found in, e.g., *C. cucullus* (see above) and two oligotrich ciliates, *Meseres corlissi* (Foissner *et al.* 2005) and *Halteria grandinella* (Foissner *et al.* 2007), when the pericyst is included in the calculations. Obviously, there is great diversity also in this feature, making it difficult to establish rules (see the “quantum” hypothesis of Ricci *et al.* 1985).

Cytochemistry

The data available on cytochemistry and biochemistry of ciliate cyst walls were excellently reviewed by Gutiérrez and Martín-González (2002) and Gutiérrez *et al.* (2003). They concluded, *inter alia*, that proteins, glycoproteins and carbohydrates are the main wall constituents. This is in accordance with the results from *M. umbrellata*: the pericyst consists of acid mucoproteins, the ectocyst possibly of carbohydrates, the mesocyst mainly of proteins, and the endocyst of glycoproteins (Figs 14–25; Table 2).

However, data on the composition of the individual cyst layers are lacking in colpodids or match the scheme mentioned above. More detailed investigations are available from stichotrichine hypotrichs, such as *Oxytricha* and *Gastrostyla*, and were collated by Delgado *et al.* (1987). Although there is a considerable diversity, some similarities and differences to *M. umbrellata* are recognizable. In both, the pericyst and ectocyst often consist of acid mucoproteins, while the mesocyst is usually composed of neutral and acid mucosubstances, rarely of proteins, as in *M. umbrellata*. The endocyst consists of glycoproteins in *M. umbrellata* (Table 2), in various *Colpoda* species, and in most or all stichotrichine hypotrichs (Delgado *et al.* 1987, Gutiérrez *et al.* 2003). Silicon (glass) is as yet unique to *M. umbrellata* (Foissner *et al.* 2009).

The cyst contents has been rarely investigated, except of the nuclear apparatus and the autophagosomes (Gutiérrez and Martín-González 2002, Gutiérrez *et al.* 2003). Usually, only (para)glycogen inclusions are mentioned. More recently, Foissner (2005) and Foissner *et al.* (2007) reported “curious” cyst inclusions in *Meseres* and *Halteria*, two oligotrich ciliates, and speculated that

they originated from the autophagosomes. These “curious structures” resemble the “spongy globules” of *M. umbrellata*, which consist of proteins and polysaccharides and are thus obviously a kind of storage product. It is strange that such composite storage bodies have been not reported from other ciliates.

Other conspicuous structures never reported before from ciliate cysts are the lipid-covered protein globules and a mass of alcian blue positive substance in the cyst plasm. Very likely, the latter material originates from the mucocysts, which are very numerous in the trophic specimen (Fig. 13) and decomposed during encystment (Foissner, unpubl.).

Functional aspects

When the cyst contents of *M. umbrellata* is cautiously squashed out, the pericyst and the ectocyst keep their sizes, while the diameter of the mesocyst and the endocyst shrinks by about 50%, without forming wrinkles (Figs 8, 11, 28). When the mesocyst splits, only the proximal part shrinks, while the distal portion remains attached to the ectocyst showing its inelasticity (Fig. 8). The elasticity of the endocyst is well known (for a review, see Gutiérrez *et al.* 2003), while that of the mesocyst seems to be a speciality of *M. umbrellata*. I cannot ascribe this feature a definite function but it shows again the high diversity of ciliate resting cysts. This conclusion is sustained when one compares detailed studies of cysts from, e.g., colpodids (*Maryna*), some oligotrichs (Foissner and Pichler 2006; Foissner *et al.* 2005, 2006, 2007, 2009), a peritrich (Calvo *et al.* 2003), and some hypotrichs (Walker and Hoffman 1985, Delgado *et al.* 1987, Foissner and Foissner 1987).

Acknowledgements. Financial support was provided by the Austrian Science Foundation, FWF project P20360-B17. The technical assistance of Mag. Birgit Weissenbacher, Mag. Gudrun Fuss, Mag. Barbara Harl, Robert Schörghofer, and Andreas Zankl is greatly acknowledged.

REFERENCES

- Akematsu T., Matsuoka T. (2005) Encystment-inducing factors in *Colpoda* sp.: cell-to-cell interaction and effect of components contained in exhausted medium. *Jpn. J. Protozool.* **38**: 53–54 (in Japanese with English summary)
- Callejas S., Gutiérrez J. C. (2003) Isolation and characterization of a cDNA encoding a putative high mobility group (HMG) – box protein from stored mRNA in resting cysts of the ciliate *Oxytricha (Sterkiella) nova*. *Mol. Biol. Rep.* **30**: 215–222
- Calvo P., Fernandez-Aliseda M. C., Garrido J., Torres A. (2003) Ultrastructure, encystment and cyst wall composition of the resting cyst of the peritrich ciliate *Opisthonecta henneguyi*. *J. Eukaryot. Microbiol.* **50**: 49–56

- Chessa M. G., Largana I., Trielli F., Rosati G., Politi H., Angelini C., Delmonte Corrado M. U. (2002) Changes in the ultrastructure and glycoproteins of the cyst wall of *Colpoda cucullus* during resting encystment. *Eur. J. Protistol.* **38**: 373–381
- Corliss J. O., Esser S. C. (1974) Comments on the role of the cyst in the life cycle and survival of free-living protozoa. *Trans. Am. microsc. Soc.* **93**: 578–593
- Delgado P., Calvo P., Torres A. (1987) Encystment in the hypotrichous ciliate *Paraurostyla weissei*: ultrastructure and cytochemistry. *J. Protozool.* **34**: 104–110
- Díaz S., Martín-González A., Rico D., Gutiérrez J. C. (2003) Morphogenesis of the division and encystment process of the ciliated protozoan *Colpoda minima*. *J. Nat. Hist.* **37**: 2395–2412
- Dunthorn M., Foissner W., Katz L. A. (2008) Molecular phylogenetic analysis of class Colpodea (phylum Ciliophora) using broad taxon sampling. *Mol. Phylogenet. Evol.* **46**: 316–327
- Endo Y., Taniguchi A. (2006) Method of chloroplast sequestration and induction of encystment in the planktonic ciliate *Strombidium conicum*. *Jpn. J. Protozool.* **39**: 53–57 (in Japanese with English summary)
- Foissner I., Foissner W. (1987) The fine structure of the resting cysts of *Kahlia simplex* (Ciliata, Hypotrichida). *Zool. Anz.* **218**: 65–74
- Foissner W. (1987) Soil protozoa: fundamental problems, ecological significance, adaptations in ciliates and testaceans, bioindicators, and guide to the literature. *Progr. Protistol.* **2**: 69–212
- Foissner W. (1991) Basic light and scanning electron microscopic methods for taxonomic studies of ciliated protozoa. *Eur. J. Protistol.* **27**: 313–330
- Foissner W. (1993) Colpodea (Ciliophora). Fischer, Stuttgart, Protozoofauna **4**: I–X + 798 pp.
- Foissner W. (2005) The unusual, lepidosome-coated resting cyst of *Meseres corlissi* (Ciliophora: Oligotricha): transmission electron microscopy and phylogeny. *Acta Protozool.* **44**: 217–230
- Foissner W. (2006) Biogeography and dispersal of micro-organisms: a review emphasizing protists. *Acta Protozool.* **45**: 111–136
- Foissner W., Pichler M. (2006) The unusual, lepidosome-coated resting cyst of *Meseres corlissi* (Ciliophora: Oligotricha): genesis of four complex types of wall precursors and assemblage of the cyst wall. *Acta Protozool.* **45**: 339–366
- Foissner W., Agatha S., Berger H. (2002) Soil ciliates (Protozoa, Ciliophora) from Namibia (Southwest Africa), with emphasis on two contrasting environments, the Etosha Region and the Namib Desert. *Denisia* **5**: 1–1459
- Foissner W., Müller H., Weisse T. (2005) The unusual, lepidosome-coated resting cyst of *Meseres corlissi* (Ciliophora: Oligotricha): light and scanning electron microscopy, cytochemistry. *Acta Protozool.* **44**: 201–215
- Foissner W., Pichler M., Al-Rasheid K., Weisse T. (2006) The unusual, lepidosome-coated resting cyst of *Meseres corlissi* (Ciliophora: Oligotricha): encystment and genesis and release of the lepidosomes. *Acta Protozool.* **45**: 339–366
- Foissner W., Müller H., Agatha S. (2007) A comparative fine structural and phylogenetic analysis of resting cysts in oligotrich and hypotrich Spirotrichea (Ciliophora). *Eur. J. Protistol.* **43**: 295–314
- Foissner W., Weissenbacher B., Krautgartner W.-D., Lütz-Meindl U. (2009) A cover of glass: first report of biomineralized silicon in a ciliate, *Maryna umbrellata* (Ciliophora: Colpodea). *J. Eukaryot. Microbiol.* (in press)
- Frenkel M. A. (1994) The cyst wall formation in *Tillina magna* (Ciliophora, Colpodidae). *Arch. Protistenk.* **144**: 17–29
- Gelei J. v. (1950) Die Marynidae der Sodagewässer in der Nähe von Szeged. *Hidrol. Közl.* **30**: 107–119
- Gutiérrez J. C., Martín-González A. (2002) Ciliate encystment-excystment cycle: a response to environmental stress. In: Microbial Development Under Environmental Stress, (Ed. J. C. Gutiérrez). Research Signpost 37/661(2), Trivandrum – 695 023, Kerala, India, 29–49
- Gutiérrez J. C., Torres A., Perez-Silva J. (1981) Excystment cortical morphogenesis and nuclear processes during encystment and excystment in *Laurentiella accuminata* (Hypotrichida, Oxytrichidae). *Acta Protozool.* **20**: 145–152
- Gutiérrez J. C., Callejas S., Borniquel S., Benítez L., Martín-González A. (2001) Ciliate cryptobiosis: a microbial strategy against environmental starvation. *Int. Microbiol.* **4**: 151–157
- Gutiérrez J. C., Díaz S., Ortega R., Martín-González A. (2003) Ciliate resting cyst walls: a comparative review. *Recent Res. Devel. Microbiol.* **7**: 361–379
- Hayat M. A. (1989) Principles and Techniques of Electron Microscopy. 3rd ed. Macmillan Press, Houndmills and London
- Janisch R. (1980) A freeze-etch study of the ultrastructure of *Colpoda cucullus* protective cysts. *Acta Protozool.* **19**: 239–246
- Jonsson P. R. (1994) Tidal rhythm of cyst formation in the rock pool ciliate *Strombidium oculatum* Gruber (Ciliophora, Oligotrichida): a description of the functional biology and an analysis of the tidal synchronization of encystment. *J. Exp. Mar. Biol. Ecol.* **175**: 77–103
- Katz L. A., McManus G. B., Snoeyenbos-West L. O., Griffin A., Pirog K., Costas B., Foissner W. (2005) Reframing the “everything is everywhere” debate: evidence for high gene flow and diversity in ciliate morphospecies. *Aquat. Microb. Ecol.* **41**: 55–65
- Kawakami H., Yagiu R. (1963) The electron microscopical study of the change of fine structure in the ciliate, *Colpoda cucullus*, during its life cycle. III. From the stage of completion of the first layer of resting cyst membrane to the completion of the resting cyst. *Zool. Mag.* **72**: 224–229
- Kim Y.-O., Taniguchi A. (1997) Seasonal variation of excystment pattern of the planktonic oligotrich ciliate *Strombidium conicum*. *Mar. Biol.* **128**: 207–212
- Lynn D. H. (2008) The Ciliated Protozoa. Characterization, Classification, and Guide to the Literature. 3rd ed. Springer, Dordrecht
- Martín-González A., Benítez L., Palacios G., Gutiérrez J. C. (1992a) Ultrastructural analysis of resting cysts and encystment in *Colpoda inflata* 1. Normal and abnormal resting cysts. *Cytobios* **72**: 7–18
- Martín-González A., Benítez L., Gutiérrez J. C. (1992b) Ultrastructural analysis of resting cysts and encystment in *Colpoda inflata* 2. Encystment process and a review of ciliate resting cyst classification. *Cytobios* **72**: 93–106
- Meier-Tackmann D. (1982) Untersuchungen über die physiologische Funktion der Cystenhülle und die Resistenz der dünnwandigen Dauercysten von *Colpoda cucullus* O. F. Müller (Holotricha, Ciliata). *Zool. Anz. Jena* **208**: 1–29
- Müller H., Wünsch C. (1999) Seasonal dynamics of cyst formation of pelagic strombidiid ciliates in a deep prealpine lake. *Aquat. Microb. Ecol.* **17**: 37–47
- Müller H., Stadler P., Weisse T. (2002) Seasonal dynamics of cyst formation of strombidiid ciliates in alpine Lake Mondsee, Austria. *Aquat. Microb. Ecol.* **29**: 181–188

- Nakamura T., Matsusaka T. (1992) Temporal suspension of encystment by salt solution in the ciliate, *Histiculus cavicola* (Kahl, 1935) (Ciliophora: Stichotrichia). *Eur. J. Protistol.* **28**: 299–304
- Oda A., Matsusaka T. (2005) Appearance and disappearance of the 140 kD protein of the ciliate, *Sterkiella cavicola*, and the ultrastructural changes of micronuclear chromatins during encystment and excystment. *Jpn. J. Protozool.* **38**: 34–35 (in Japanese with English summary)
- Pearse A. G. (1968) Histochemistry, Vol. 1. 3rd ed. J. & A. Churchill, London
- Ricci N., Verni F., Rosati G. (1985) The cyst of *Oxytricha bifaria* (Ciliata: Hypotrichida). I. Morphology and significance. *Trans. Am. microsc. Soc.* **104**: 70–78
- Romeis B. (1968) Mikroskopische Technik. 16th ed. R. Oldenbourg Verlag, München, Wien
- Ruthmann A., Kuck A. (1985) Formation of the cyst wall of the ciliate *Colpoda steinii*. *J. Protozool.* **32**: 677–682
- Sugimoto H., Endoh H. (2008) Differentially expressed genes during fruiting body development in the aggregative ciliate *Sorogena stoianovitchae* (Ciliophora: Colpodea). *J. Eukaryot. Microbiol.* **55**: 110–116
- Tibbs J. (1968) Fine structure of *Colpoda steinii* during encystment and excystment. *J. Protozool.* **15**: 725–732
- Tsutsumi S., Watoh T., Kumamoto K., Kotsuki H., Matsuoka T. (2004) Effects of porphyrins on encystment and excystment in ciliated protozoan *Colpoda* sp. *Jpn. J. Protozool.* **37**: 119–126
- Wagtendonk W. J. van (1955) Encystment and excystment of Protozoa. In: Biochemistry and Physiology of Protozoa, (Eds. S. H. Hutner, A. Lwoff). Academic Press, New York, 85–90
- Walker G. K., Hoffman J. T. (1985) An ultrastructural examination of cyst structure in the hypotrich ciliate *Gonostomum* species. *Cytobios* **44**: 153–161
- Watoh T., Yamaoka M., Nagao M., Oginuma K., Matsuoka T. (2003) Inducing factors for encystment and excystment in ciliated protozoan *Colpoda* sp. *Jpn. J. Protozool.* **36**: 105–111 (in Japanese with English summary)

Received on 14th May, 2009; accepted on 11th June, 2009